A power plant for integrated waste energy recovery from liquid air energy storage and liquefied natural gas

Zhang, Tongtong; She, Xiaohui; Ding, Yulong

DOI:
10.1016/j.cjche.2021.02.008

A power plant for integrated waste energy recovery from liquid air energy storage and liquefied natural gas

Tongtong Zhang[1*], Xiaohui She[1], Yulong Ding[1*]

[1]Birmingham Centre for Energy Storage, School of Chemical Engineering, University of Birmingham, Birmingham, B15 2TT, UK

*Corresponding author: Yulong Ding, PhD; Email: y.ding@bham.ac.uk

Tongtong Zhang; Email: txz772@student.bham.ac.uk

Abstract

Liquefied Natural Gas (LNG) is regarded as one of the cleanest fossil fuel and has experienced significant developments in recent years. The liquefaction process of natural gas is energy-intensive, while the regasification of LNG gives out a huge amount of waste energy since plenty of high grade cold energy (-160 ºC) from LNG is released to sea water directly in most cases, and also sometimes LNG is burned for regasification. On the other hand, Liquid Air Energy Storage (LAES) is an emerging energy storage technology for applications such as peak load shifting of power grids, which generates 30-40% of compression heat (~200 ºC). Such heat could lead to energy waste if not recovered and used. The recovery of the compression heat is technically feasible but requires additional capital investment, which may not always be economically attractive. Therefore, we propose a power plant for recovering the waste cryogenic energy from LNG regasification and compression heat from the LAES. The challenge for such a power plant is the wide working temperature range between the low-temperature exergy source (-160 ºC) and heat source (~200 ºC). Nitrogen and argon are proposed as the working fluids to address the challenge. Thermodynamic analyses are carried out and the results show that the power plant could achieve a thermal efficiency of 27% and 19% and an exergy efficiency of 40% and 28% for nitrogen and argon, respectively. Here, with the nitrogen as working fluid undergoes a complete Brayton Cycle, while the argon based power plant goes through a combined Brayton and Rankine Cycle. Besides, the economic analysis shows that the payback period of this proposed system is only 2.2 years, utilizing the excess heat from a 5MW/40MWh LAES system. The findings suggest that the waste energy based power plant could be co-located with the LNG terminal and LAES plant, providing additional power output and reducing energy waste.

Keywords: Waste energy recovery, Power plant, Liquid air energy storage, Liquefied Natural Gas, Integration

Nomenclature		C	*Capital cost* ($)
h	Specific enthalpy (kJ/kg)	NPV	Net present value ($)
m	Mass flow rate (kg/s)	SIR	Saving to investment ratio
K	Mass flow rate ratio	*lifetime*	Lifespan, year
P	Pressure (MPa)	r	Discount rate
T	Temperature (K)	***Subscripts/Superscripts***	
s	Specific entropy (kJ/(kg·K))	i	Status
W	Power consumption/generation (kW)	s	Isentropic process
w_{net}	Specific power generation (kJ/kg)	*com*	Compressor/pump
Q_{hot}	Heat input (kW)	*turb1*	Turbine#1
Ex	Exergy flow rate (kW)	*turb2*	Turbine#2
ex	Specific exergy (kJ/kg)	*cryo-pump*	Cryo-pump
Ex_{in}	Exergy input (kW)	*HEX1*	Heat exchanger#1
Ex_{d}	Exergy destruction (kW)	*HEX2*	Heat exchanger#2
η	Isentropic efficiency	*AHEX*	Ambient heat exchanger
η_{th}	Thermal efficiency	*PG1*	Power generation#1
η_{ex}	Exergy efficiency	*PG2*	Power generation#2
Δt	Temperature difference (K)	*WF*	Working fluid (nitrogen/argon)
q_{HX}	Heat flux of heat exchanger (W)	*oil*	Thermal oil
htc	Heat transfer coefficient	*LNG*	LNG
$CEPCI$	Chemical engineering plant cost index	ambient	Ambient
C_{NCI}	Net cash inflow ($)	in/out	Inlet/outlet
C_{revenue}	Revenue obtained ($)	c	Cold side
$C_{\mathrm{O\&M}}$	Operating and maintenance cost ($)	h	Hot side

1. Introduction

In the past few decades, there has been a significant growth in the utilization of clean energy resources to fight against global warming and related problems. Natural gas (NG), as one of the cleanest fossil fuels, attracts more and more attention in recent years as a result and becomes one of the fastest growing non-renewable energy sources following coal. NG has a very high calorific value with low environmental pollution and has been widely used across the world. NG production has enjoyed a 4% per year growth between 2005 and 2015 and the projected increase in world NG consumption can reach nearly 43% from 2015 to 2040 [1]. However, the distribution for the NG is geographically uneven with long-distance transportation required for NG trading. NG has three main forms during transportation from the NG exporting countries to the NG consumers: piped NG (PNG) through pipelines, compressed NG (CNG) in gas cylinders, and liquefied NG (LNG) in cryogenic tankers [2]. For places unconnected to global NG pipeline networks, LNG is a preferred form because of reduced storage volume of NG by ~600 times through liquefaction [2,3]. The world LNG trade is expected to triple to ~31 trillion cubic feet, from 2015 to 2040 [1].

The liquefaction process of NG is the most energy-intensive step in the LNG value chain[3]. The process consumes electricity to drive a refrigeration cycle for liquifying NG. When LNG is used, it needs to be heated by a heat source, such as seawater and burning NG, for regasification normally, as shown in Fig. 1 (a). The required distribution pressure of natural gas depends on the consumption purposes, which is about 3-70 MPa for local distribution and long-distance transmission [4]. A large amount of cold energy in LNG is therefore wasted if there is no recovery step during the regasification process. This calls for a sustainable way to recover and reuse such a high grade cold energy. There are several traditional ways which could extract energy from cryogens, such as direct expansion method, Rankine Cycle method, Brayton cycle method, and Combined method [5]. In recent years, some attention has been drawn to the cold energy recovery of LNG using Liquid Air Energy Storage (LAES) system.

LAES is a large-scale energy storage technology. The key features of such a technology lie in high energy storage density, long lifespan, low capital cost, and no geographic limitation, etc. [6]. The storage medium of the LAES is the liquid air or liquid nitrogen, which is easy to obtain and pollution-free [7,8]. The principle of the LAES is shown in Fig. 1 (b). At off-peak times, the LAES system is charged through air liquefication. Such a process involves compression and cooling during which compression heat can be recovered and stored. And at peak times, the discharging process of the LAES system occurs through power generation, during which the stored compression heat can be used to heat the air before expansion. However, the round-trip efficiency (< 60 % for a stand-alone LAES system) is often regarded as an issue [9]. The enhancement of the LAES efficiency through integration with the LNG recovery process offers a potentially effective solution.

Peng et al. [10] proposed a system design, denoted as LAES-LNG-CS, where the cold energy released during the regasification process of LNG is recovered and stored in pressurized propane. The stored cold energy is reutilized in the cold box of the LAES system through cooling down compressed air, thus improving the liquid yield of the LAES charging process. The advantage of this LAES-LNG-CS system is that a cryogenic storage unit is used to link the LAES system and the LNG terminal, which makes the LNG regasification process works independently from the LAES system. Also, the round-trip efficiency of the LAES-LNG-CS system could reach ~88%. Park et al. [11] proposed an integration method (denoted as MCES) which is a bit similar to the system proposed in [10]. The main difference is that Park et al. proposed that the cold energy of LNG could be either recovered and stored in a cryogenic unit for further use or utilized to liquify the compressed air directly without storage. This MCES could obtain a round-trip efficiency of 85.1%. Besides, Park et al. [12,13] also proposed another way to integrate the LAES system with the LNG regasification power plant (called LPCES). The LPCES system has three different working modes corresponding to different working hours. During off-peak period, the LAES is charged, whilst the LNG is introduced to the cold box of the LAES system to directly cool down the compressed air. During peak period, the LNG is introduced to a common regasification power unit for power generation and the LAES discharges. During non-peak and non-off-peak periods, the LAES system is switched off and the LNG is used to drive the normal regasification power unit. A very high round-trip efficiency of 95.2% could be achieved, whereas the regasification power unit needs to start and stop frequently, making this system difficult to operate practically. Whichever way it is use to recover the cold energy of LNG, the cold energy is finally used to cool down and liquify the air which has been already compressed to high pressure by multi-stage compressors in [11–13]. However, Park et al. [14] proposed a new method to utilize the cold energy of LNG in LAES system, in which the cold energy of LNG is used to cool down the air before the air entering every single stage of compressors, reducing the power consumption for air compression. Zhang et al [15] studied the recovery of cold energy of LNG in the cold box to cool down the compressed air directly without using the cryogenic storage unit. Besides, external heat is also introduced for power generation enhancement and a round-trip efficiency of ~70.5% was obtained. A similar method to recover the cold energy of LNG based on the LAES system but without any external heat is proposed by Li et al. [16], which obtained a round-trip efficiency of ~60%. Kim et al. [17] proposed an integrated system to combine both the LNG regasification process and the NG combustion process with the LAES system. During discharging process, the cold energy of both LNG and liquid air can be recovered and stored for later use in the liquefication process of the LAES to produce liquid air. The difference of this integrated system is that after such a cold recovery process, the gaseous air and NG are mixed and combusted to drive a Brayton Cycle for power generation, achieving a round-trip efficiency of 64.2%. Hamdy et al. [18] compared different integrated methods between the LAES system and NG combustion/LNG/waste heat. Their economic analysis showed that the most economically feasible configuration could be achieved when double combustion chambers are employed where the NG could be burned to increase the turbine inlet temperature during discharging process. The Levelized Cost of Electricity (LCOE) of the LAES with the combustion chamber and LNG cold energy recovery together is much lower than that of the LAES with LNG cold energy recovery only. A novel system design (called LNG-CES) is proposed by Lee et al. [19], in which both the thermal component and the pressure component of the LNG cold energy are used to drive the charging process of the LAES system to produce liquid air without consuming external electricity. When electricity is needed, the cold energy of LNG can be recovered for power generation through pressurizing, heating, and expanding the liquid air. The exergy efficiency of the energy storage process and energy recovery process could attain 94.2% and 61.1%, respectively. Whereafter, to make the LNG-CES system more efficient and more industrially feasible, two improved system designs are proposed. An Organic Rankine Cycle is added in this LNG-CES system (called LNG-ORC-LAES) for additional power generation which could increase the efficiency further [20]. More practical components are applied in LNG-CES system [21], such as expansion valve and vapor-liquid separator etc., thus improving the practicability of this system greatly.

From the above literature review, which has been summarized in Table 1, it could be found that almost all the related research about the LNG cold energy recovery process integrated with the LAES

Table 1 Main features of integration of LAES with LNG regasification process in literature

LAES Configurations	LNG regasification working mode	Liquid air storage pressure	LAES working mode	Research method	Ref.
Conventional LAES system	Full time: LNG evaporated with cold energy recovered and stored in LAES cold storage tank	0.1 MPa	Off-peak: air liquefaction/charging with stored cold as cold load Peak: power generation/discharging with stored heat for air heating	Thermodynamic simulation	Peng et al. 2019 [10]
Conventional / modified LAES system	Off-peak: LNG evaporated in LAES cold box for refrigeration Other time: no description	0.1-0.2 MPa	Off-peak: air liquefaction/charging with LNG and stored cold as cold load Peak: power generation/discharging with stored/external heat for air heating	Thermodynamic simulation	Zhang et al. 2018 [15] Li et al. 2017 [16]
Conventional / modified LAES system	Off-peak: LNG evaporated in LAES cold box for refrigeration Peak-time: NG combusted with air for power generation	0.1 MPa	Off-peak: air liquefaction/charging with LNG and stored cold as cold load Peak: power generation/discharging with stored heat or waste heat or NG combustion for air heating	Thermodynamic / economic simulation	Hamdy et al. [18]
Modified LAES system	Peak-time: LNG evaporated with cold energy recovered and stored in cold storage tank, and NG combusted with air for power generation Other time: not working	0.2 MPa	Off-peak: air liquefaction/charging with stored cold as cold load Peak: power generation/discharging with gas turbine driven by combusted gas (re-gasified air and NG burned)	Thermodynamic / economic simulation	Kim et al. 2018 [17]
Modified LAES system	Off-peak: LNG evaporated in LAES cold box for refrigeration Other time: LNG evaporated with cold energy recovered and stored in cold storage tank	3.7 MPa	Off-peak: air liquefaction/charging with LNG and stored cold as cold load Peak: power generation/discharging at ambient temperature	Thermodynamic simulation	Park, You et al. 2020 [11]

Modified LAES system	Off-peak: LNG evaporated in LAES cold box for refrigeration Other time: LNG evaporated without integrated with LAES	~2.5 MPa	Off-peak: air liquefaction/charging with LNG as cold load Peak: power generation/discharging at ambient temperature	Thermodynamic simulation	Park et al. 2017 [12-13]
Modified LAES system	Off-peak: LNG evaporated in LAES heat exchangers for intercooling Other time: LNG evaporated with cold energy recovered and stored in cold storage tank	3.7 MPa	Off-peak: air liquefaction/charging with LNG and stored cold as cold load Peak: power generation/discharging at ambient temperature	Thermodynamic / economic simulation	Park, Cho et al. 2020 [14]
Modified LAES system	Full time: LNG evaporated in LAES heat exchangers for intercooling, and ORC and direct expansion driven by NG to provide energy for air compression	21 MPa	Full time: air liquefaction/charging with LNG as cold load and NG expansion as power input Peak: power generation/discharging at ambient temperature	Thermodynamic simulation / economic simulation	Lee, Park et al. 2017 [19] Lee, You et al. 2019 [20]
Modified LAES system	Full time: LNG evaporated in LAES heat exchangers for intercooling, and NG expanded to provide energy for air compression	1.8 MPa	Full time: air liquefaction/charging with LNG as cold load and NG expansion as power input Peak: power generation/discharging at ambient temperature	Thermodynamic simulation	Lee, Park et al. 2019 [21]
Conventional LAES system	Full time: LNG evaporated with cold energy recovered and stored in separate cold storage tank	0.1 MPa	Off-peak: air liquefaction/charging with stored cold as cold load Peak: power generation/discharging with stored heat for air heating + with Brayton cycle driven by stored LNG cold and LAES excess heat	Thermodynamic simulation	She et al. 2019 [22]

system is utilizing the cold energy of LNG to optimize the air liquefication process of the LAES system. Through the integration with the cold energy recovery of LNG, the liquid yield of the charging process of the LAES system could increase obviously, and in turn, the efficiency of the whole system could be improved. However, almost all these system designs need to change the existing structure of the LAES system through either adding extra cryogenic storage units or updating the original cold box, and some even change the LAES basic configurations completely, which increases practically technical difficulties. Thus, most of the studies about the integration of the LAES system with LNG regasification process still stay in theoretical research stage and have a long way to be put into practice.

According to the finding in [23–25] about 15-45% of the compression heat recovered in the charging process of the LAES system could not be fully used in the discharging process, shown in Fig. 2. This part of excess compression heat (~460-500 K) needs to be either employed elsewhere or released to the ambient directly. Thus, our group [22] proposed to utilize the excess compression heat to drive a Brayton Cycle with the LNG cold energy together (denoted as LAES-Brayton-LNG), in which nitrogen is selected as the working fluid. In this way, the amount of power generation of the LAES could be greatly enhanced, and the round-trip efficiency could be further improved to 72%. The most significant advantage of the LAES-Brayton-LNG system is that there is no change of the current configurations of the LAES system and the LNG regasification process, making it much more easily applied widely. Since LNG regasification is a very important industrial process and has been developed for decades, there have been many LNG regasification terminals across the world already. However, the LAES is still a developing energy storage technology, and commercialization of the LAES technology is ongoing. There are an LAES pilot plant (350 kW/2.5 MWh) and a grid-scale LAES demonstrator plant (5 MW/15 MWh) developed and tested successfully and a 50 MW LAES facility being constructed. The LAES-Brayton-LNG system could remain the current configurations of both the regasification process and the LAES system, which provides a guidance for investors to build a new LAES power plant nearby an existing LNG terminal. There is very less need to reconstruct the original configurations of the LNG terminal, and the current LAES system design could be adopted to use ‘off the shelf’ components as much as possible, reducing the cost of investment and increasing the both the commercial and technical feasibility. However, our previous research [22] mainly focused on the thermodynamic analysis of the overall system, while very little work has been done to optimize the performance of the newly proposed

Brayton Cycle, which is the core of this LAES-Brayton-LNG system actually.

Thus, this paper aims to bridge this gap by doing performance optimization on the proposed power plant based on waste energy recovery. Both the high grade cold energy released from the LNG regasification process and the excess compression heat energy obtained from the LAES system are utilized to drive the power plant as the low-temperature exergy source and heat source, respectively. Besides, two working fluids, nitrogen, and argon are selected in this power generation system for comparison purpose. Both energy analysis and exergy analysis based on these two working fluids are carried out on this proposed system under different working conditions (including constant/limited low-temperature exergy source and constant/limited heat source), which helps to find out the optimal operating parameters. These findings will provide a guideline for designing power plants working in a wide temperature range, especially for recovering LNG cryogenic energy and industrial waste heat.

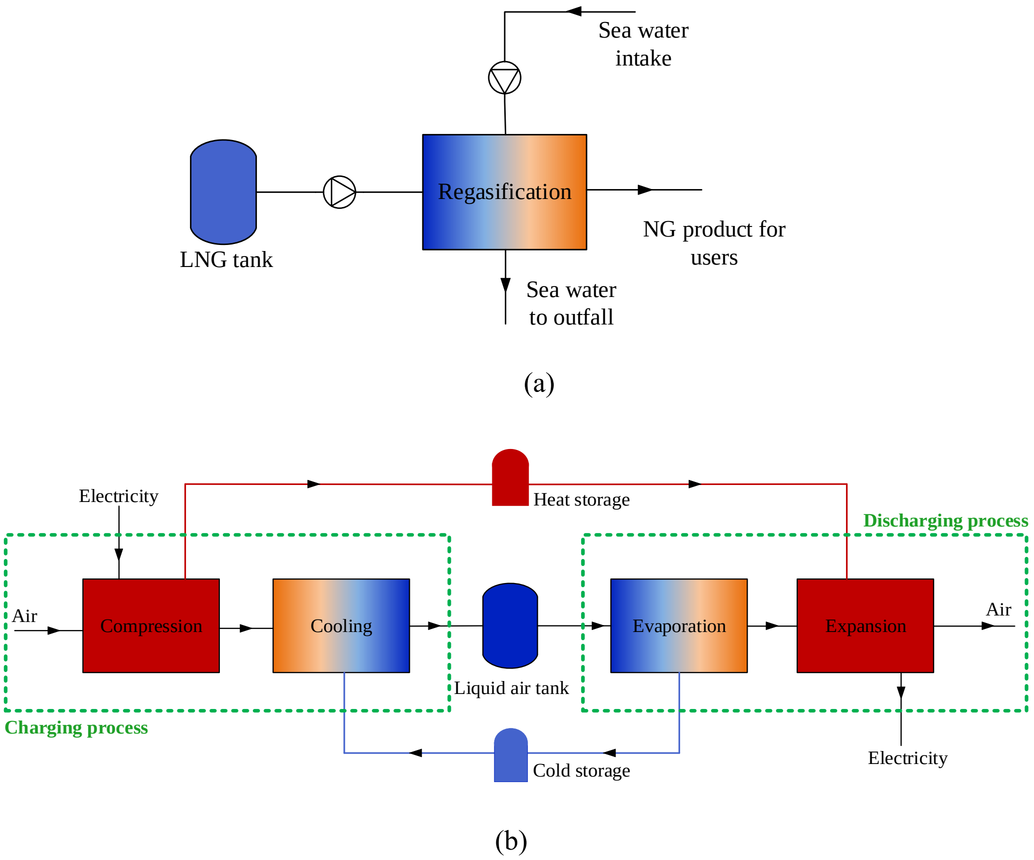

Fig. 1. Schematic diagrams of the basic principle of LNG regasification process (a) and LAES (b)

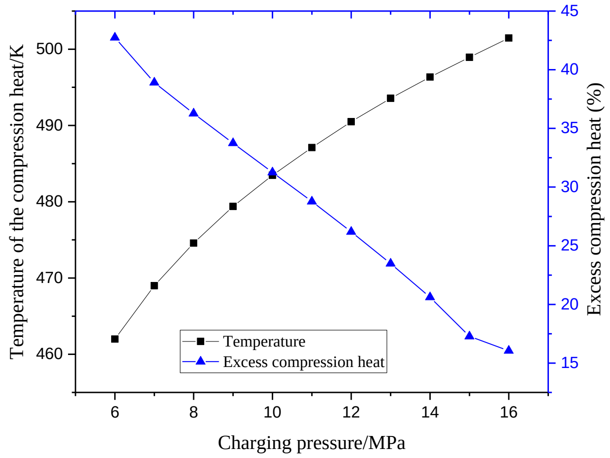

Fig. 2 Excess compression heat (hot thermal oil) in the LAES with different charging pressure

2. System description and methodology

2.1 System description

As is described above, the compression heat which is recovered and stored in the thermal oil is surplus in the stand-alone LAES system. Thus, this part of the high-temperature thermal oil could be used with the pressurized LNG together to drive a power generation cycle (Brayton or Rankine Cycle), hence producing more electricity, and improving the round-trip efficiency. Fig. 3(a) shows this proposed power generation system, consisting of two power generation cycles: Power generation #1 and #2. In Power generation #1, the high-temperature compression heat from the LAES system and the high-grade cold energy of LNG are integrated, working as the hot source and cold source, respectively. Power generation #2 is the traditional LNG direct expansion cycle.

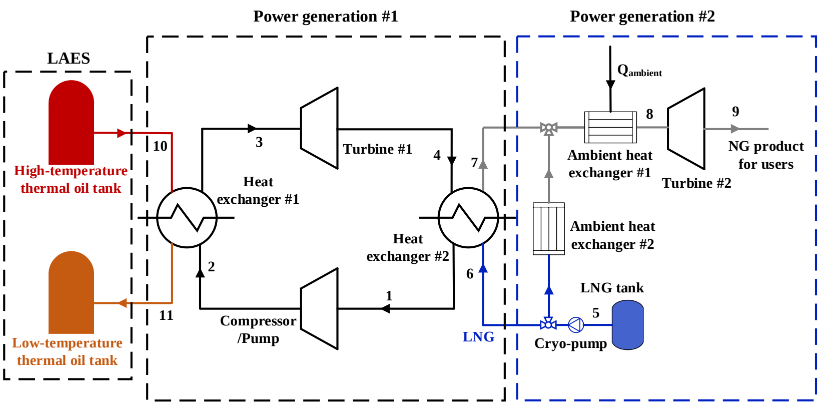

(a)

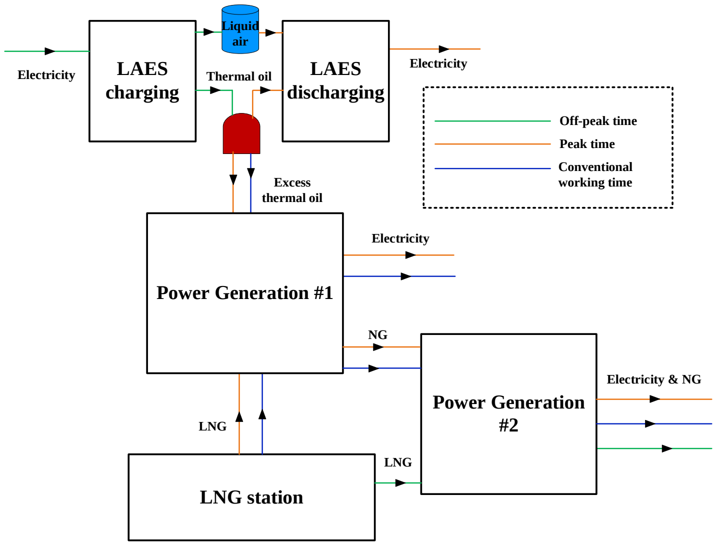

(b)

Fig. 3. (a) Flowsheet of the proposed power generation system, and (b) working mode of the proposed power generation system

The excess compression heat from LAES could be utilized in a very flexible way in the proposed power generation system, as shown in Fig. 3(b), depending on both the user demand of NG and the working time of LAES charging process:

During off-peak time, the LAES system works in charging process to produce the high-temperature thermal oil. Thus, when NG is in demand during this period, the LNG could be pumped out and heated for regasification through the original LNG regasification equipment (ambient heat exchanger #1 and 2), and finally expanded to the required pressure, driving the turbine #2 for power generation, which is the same as common LNG terminals. The required pressure of NG product for users depends on the purpose, as illustrated in Table 2. In this paper, NG product is assumed to be used for long distance transmission.

During peak time, the LAES system works in discharging process for power generation. When NG is in demand during this period, both the Power generation #1 and Power generation #2 work for LNG regasification and extra electricity generation. In Power generation #1, the working fluid is compressed by the compressor firstly (Status 2). Then it is heated up through the heat exchange with a stream of the high-temperature thermal oil from the LAES system (Status 3). The high-temperature compressed working fluid then expands in the turbine#1 for power generation (Status 4), after which, the working fluid is cooled down (Status 1) through the heat exchange with the pressurized LNG. Meanwhile, the pressurized LNG could finish the first regasification process in heat exchanger #2 from Status 6 to

Status 7. Finally, the working fluid is compressed to high pressure (Status 2) again to complete the whole closed cycle. In Power generation #2, the pressurized NG from the outlet of heat exchanger #2 (Status 7) enters the ambient heat exchanger for further regasification (Status 8), after which, the high-pressure NG expands directly in the turbine#2 to the gas-supplying pressure (Status 9) for more power generation. Through this combined power generation system, the LNG could complete its regasification process with less waste of the high grade cold energy, and the obtained NG is supplied to users through pipelines.

During conventional working period (non peak time and non off-peak time), the LAES system stops working. If there is still excess thermal oil left in the high-temperature thermal oil storage tank, the Power generation #1 and Power generation #2 could operate the same way as at the peak time, until the thermal oil is run out. After that, the Power generation #1 stops running and only the Power generation #2 keeps working for LNG regasification.

Table 2 Required pressure of NG for several purposes [4]

Purpose	Pressure (MPa)
Steam power stations	0.6
Combined cycle stations	2.5
Local distribution	3
Long distance transmission	7

Thus, according to the system described above, it could be seen that this proposed power generation system could recover the waste energy from the LAES system and NG supply terminal without changing the system structure and components of the existing LAES system.

2.2 System model development

2.2.1 Energetic analysis

In Power generation #1 of this power generation system, the working fluid is compressed to high pressure, and the outlet enthalpy of the working fluid after the compression process could be calculated as follow:

$$h_2 = h_1 + \frac{(h_{2,s} - h_1)}{\eta_{com}} \tag{1}$$

Then the pressurized working fluid (Status 2) is heated up by the high-temperature thermal oil in heat exchanger #1. The outlet state (Status 3) can be calculated according to the law of energy conservation and the limitation of the pinch point:

$$m_{WF} \cdot (h_3 - h_2) = K_{oil} \cdot m_{WF} \cdot (h_{10} - h_{11}) \tag{2}$$

$$K_{oil} = \frac{m_{oil}}{m_{WF}} \tag{3}$$

The high-temperature pressurized working fluid (Status 3) then expands in the turbine #1 to low pressure (Status 4), and the outlet condition can be obtained through the formula shown below:

$$h_4 = h_3 - \eta_{turb1} \cdot (h_3 - h_{4,s}) \tag{4}$$

The working fluid out of the turbine (Status 4) is cooled down by the pressurized LNG. The outlet state of the working fluid (Status 1) can be figured out depending on the law of energy conservation and the limitation of the pinch point:

$$m_{WF} \cdot (h_4 - h_1) = K_{LNG} \cdot m_{WF} \cdot (h_7 - h_6) \tag{5}$$

$$K_{LNG} = \frac{m_{LNG}}{m_{WF}} \tag{6}$$

In Power generation #2 of this power generation system, the ambient-pressure LNG (Status 5) which is stored in the LNG tank is pumped to high pressure (Status 6) by the cryo-pump, and the cryo-pump outlet condition of the LNG could be calculated as follow:

$$h_6 = h_5 + \frac{(h_{6,s} - h_5)}{\eta_{\text{cryo-pump}}} \tag{7}$$

The pressurized LNG would be heated to ambient temperature in the ambient heat exchanger after finishing the first regasification process Power generation #1:

$$T_8 = T_{\text{ambient}} \tag{8}$$

$$Q_{\text{ambient}} = m_{LNG} \cdot (h_8 - h_7) \tag{9}$$

The ambient-temperature pressurized NG (Status 8) then expands in the turbine #2 to gas-supplying pressure (Status 9), and the outlet condition can be obtained through the formula shown below:

$$h_9 = h_8 - \eta_{turb2} \cdot (h_8 - h_{9,s}) \tag{10}$$

The specific power generation of this proposed power generation system, w_{net}, is defined as the net energy output produced by per unit mass flow of the working fluid, which is the sum of the specific power generation of Power generation #1 ($w_{net,PG1}$) and #2 ($w_{net,PG2}$):

$$w_{net} = w_{net,PG1} + w_{net,PG2} = \frac{W_{turb1} - W_{com}}{m_{WF}} + \frac{W_{turb2} - W_{cryo-pump}}{m_{WF}} \tag{11}$$

$$W_{com} = m_{WF} \cdot (h_2 - h_1) \tag{12}$$

$$W_{turb1} = m_{WF} \cdot (h_3 - h_4) \tag{13}$$

$$W_{cryo-pump} = m_{LNG} \cdot (h_6 - h_5) \tag{14}$$

$$W_{turb2} = m_{LNG} \cdot (h_8 - h_9) \tag{15}$$

The power generation per unit mass flow of LNG (w_{net}^{LNG}) and per unit mass flow of the thermal oil (w_{net}^{oil}) are defined respectively as:

$$w_{net}^{LNG} = w_{net,PG1}^{LNG} + w_{net,PG2}^{LNG} = \frac{W_{turb1} - W_{com}}{m_{LNG}} + \frac{W_{turb2} - W_{cryo-pump}}{m_{LNG}} \tag{16}$$

$$w_{net}^{oil} = w_{net,PG1}^{oil} + w_{net,PG2}^{oil} = \frac{W_{turb1} - W_{com}}{m_{oil}} + \frac{W_{turb2} - W_{cryo-pump}}{m_{oil}} \tag{17}$$

Then the thermal efficiency of this proposed system, η_{th}, is defined as the ratio of the net energy output of this system to the total heat input at the high temperature of this system:

$$\eta_{th} = \frac{(W_{turb1} - W_{com}) + (W_{turb2} - W_{cryo-pump})}{Q_{hot,PG1} + Q_{hot,PG2}} \tag{18}$$

$$\eta_{th,PG1} = \frac{(W_{turb1} - W_{com})}{Q_{hot,PG1}} \tag{19}$$

$$Q_{hot,PG1} = m_{oil} \cdot (h_{10} - h_{11}) \tag{20}$$

$$Q_{hot,PG2} = Q_{\mathrm{ambient}} \tag{21}$$

2.2.2 Exergetic analysis

In this study, the exergy flow rate is defined as the product of the mass flow rate and the specific exergy (ignoring the kinetic and potential exergy), which could be calculated by:

$$Ex_i = m_i \cdot ex_i = m_i \cdot [(h_i - h_{\text{ambient}}) - T_{\text{ambient}} \cdot (s_i - s_{\text{ambient}})] \tag{22}$$

The exergy input by the LNG to the whole system and the Power generation #1 could be given:

$$Ex_{\text{in}}^{LNG} = Ex_5 - Ex_9 \tag{23}$$

$$Ex_{\text{in,PG1}}^{LNG} = Ex_6 - Ex_7 \tag{24}$$

The exergy input by the thermal oil to the system is given:

$$Ex_{\text{in}}^{oil} = Ex_{10} - Ex_{11} \tag{25}$$

Thus, the total exergy input to the whole system and Power generation #1 are:

$$Ex_{\text{in}} = Ex_{\text{in}}^{LNG} + Ex_{\text{in}}^{oil} \tag{26}$$

$$Ex_{\text{in,PG1}} = Ex_{\text{in,PG1}}^{LNG} + Ex_{\text{in}}^{oil} \tag{27}$$

There are several different definitions of exergy efficiency proposed by different authors [26,27]. The exergy efficiency of the system is defined as the ratio of the total useful exergy output of the system to the total exergy input of the system, in which the net power output of the system is considered as the useful exergy output, while the physical exergy changes of the natural gas and the thermal oil are considered as the exergy input. This exergy efficiency definition in this paper is very common and has been used in many studies about the LNG-based power generation system [28–30].

$$\eta_{ex} = (m_{WF} \cdot w_{net}) / Ex_{\text{in}} = (Ex_{\text{in}} - Ex_{\text{d}}) / Ex_{\text{in}} \tag{28}$$

$$\eta_{ex,PG1} = (m_{WF} \cdot w_{net,PG1}) / Ex_{\text{in,PG1}} = (Ex_{\text{in,PG1}} - Ex_{\text{d,PG1}}) / Ex_{\text{in,PG1}} \tag{29}$$

in which, Ex_{d} and $Ex_{\text{d,PG1}}$ represent the total exergy destruction of the whole system and the Power generation #1. The total exergy destruction is the sum of the exergy destruction on each system component:

$$Ex_{\text{d}} = Ex_{\text{d}}^{com} + Ex_{\text{d}}^{HEX1} + Ex_{\text{d}}^{turb1} + Ex_{\text{d}}^{HEX2} + Ex_{\text{d}}^{cryo-pump} + Ex_{\text{d}}^{AHEX} + Ex_{\text{d}}^{turb2} \tag{30}$$

$$Ex_{\text{d,PG1}} = Ex_{\text{d}}^{com} + Ex_{\text{d}}^{HEX1} + Ex_{\text{d}}^{turb1} + Ex_{\text{d}}^{HEX2} \tag{31}$$

$$Ex_{\text{d}}^{com} = Ex_1 - Ex_2 + W_{com} \tag{32}$$

$$Ex_{\text{d}}^{HEX1} = Ex_2 - Ex_3 + Ex_{10} - Ex_{11} \tag{33}$$

$$Ex_{\mathrm{d}}^{turb1} = Ex_3 - Ex_4 - W_{turb1} \tag{34}$$

$$Ex_{\mathrm{d}}^{HEX\,2} = Ex_4 - Ex_1 + Ex_6 - Ex_7 \tag{35}$$

$$Ex_{\mathrm{d}}^{cryo-pump} = Ex_5 - Ex_6 + W_{cryo-pump} \tag{36}$$

$$Ex_{\mathrm{d}}^{AHEX} = Ex_7 - Ex_8 \tag{37}$$

$$Ex_{\mathrm{d}}^{turb2} = Ex_8 - Ex_9 - W_{turb2} \tag{38}$$

2.3 Economic performance indexes

To evaluate the economic benefit of this proposed power generation system, an economic analysis is performed. The net present value (*NPV*) and saving to investment ratio (*SIR*) to invest this power generation system are investigated to suggest the investors whether the investment of such a power plant based on waste heat will be cash-flow-positive. *NPV* is defined as the difference between the present value of revenue and the present value of cost. *SIR* is calculated by dividing the present value of revenue by the present value of cost. *NPV*>0 and *SIR*>1 indicate that the investment has a potential economic benefit, otherwise, it suggests an economic loss.

$$NPV = \sum_{i=1}^{lifetime} \frac{C_{NCI}}{(1+r)^i} - C \tag{39}$$

$$C_{NCI} = C_{\mathrm{revenue}} - C_{O\&M} \tag{40}$$

$$SIR = \frac{\sum_{i=1}^{lifetime} \frac{C_{NCI}}{(1+r)^i}}{C} \tag{41}$$

Besides, the payback period is also an important index to evaluate the economic value of an investment, which is defined as below:

$$payback\_period = \frac{C}{C_{NCI}} \tag{42}$$

2.4 Model validation

The reasonability of the system model has a key influence on the accuracy of the following thermodynamic analysis. Thus, it is very necessary to validate this model first before further calculation and discussion. The power generation system model built for this study is compared to the operating date got from Chena Geothermal Power Plant which is located in Chena, Alaska, USA. Chena Geothermal Power Plant is a power station using the Organic Rankine Cycle (ORC) unit to generate electricity, of which the capacity can reach 250 kW. The heat source of this ORC power plant is the low-temperature geothermal heat source (geothermal hot water/steam). Ambient-temperature cooling water is used to condense the working fluid (R134a). The process flow diagram and detailed operation conditions of this Chena Geothermal Power Plant [31] are shown in Fig. 4 and Table 3 respectively, which this validation is designed following. The comparison results of the simulation results with the real operating data [31] are listed in Table 4. From the comparison, it could be observed that the maximum deviation is 3.29%, illustrating that the simulation results can match well with the real data of the power station. Thus, the model of this power generation system is reasonable and can be used for the following calculation and analysis.

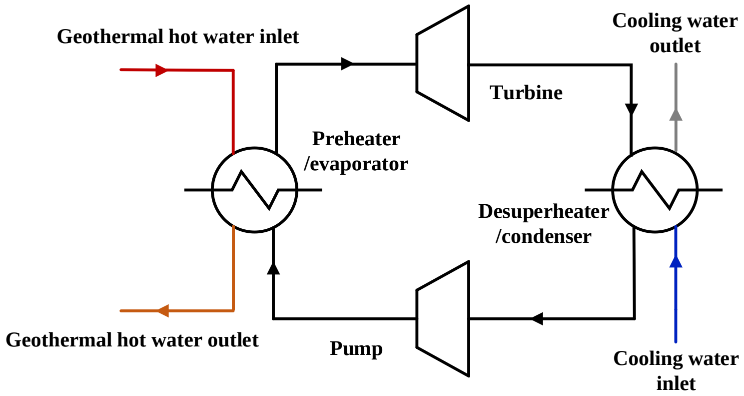

Fig. 4 Process flow diagram of Chena Geothermal Power Plant

Table 3 Design conditions for the power generation system [31]

Parameters	Value
Working fluid	R134a
Mass flow rate of the working fluid (kg/s)	12.2
Mass flow rate of the cooling water (kg/s)	101.7
Inlet temperature of the cooling water (K)	277.6
Mass flow rate of the geothermal fluid (kg/s)	33.4
Inlet temperature of the geothermal fluid (K)	346.5
Turbine efficiency	80%
Pump efficiency	75%
Inlet pressure of the turbine (MPa)	1.6
Outlet pressure of the turbine (MPa)	0.44

Table 4 Model validation results

Parameters	Simulation result	Real power station data [31]	Relative error
Outlet temperature of the geothermal fluid	331.4 K	327.6 K	1.16%
Outlet temperature of the cooling water	282.1 K	282.9 K	0.28%
Output power of the turbine	251.5 kW	250 kW	0.60%
Net power of the system	216.9 kW	210 kW	3.29%

3. Results and discussion

Many factors could influence the performance of this power generation system, among which, the pressure ratio of the turbine, the temperatures of the cold and heat sources, and the ratio of the mass flow rates among the working fluid, cold fluid, and hot fluid are the most critical parameters. Thus, the research is developed from these key influence factors and focuses on the analysis of how these factors affect the thermodynamic characters of this proposed system. Matlab is used to calculate system performance. Besides, the thermal properties of nitrogen, argon, and LNG (assumed to be pure methane) are obtained by using REFPROP 8.1, and the thermal properties of thermal oil from ASPEN plus.

Table *5* lists the default operating conditions used for the simulation of this power generation system. The calculation results and a comprehensive discussion of these results will be present in this section.

Table 5 Default design conditions for the power generation system

Parameters	Value
Thermal oil temperature (K)	473.15
LNG temperature (K)	111.51
LNG pressure in tank (MPa)	0.1
Cryo-pump outlet temperature of LNG (K)	116.94
Cryo-pump outlet pressure of LNG (MPa)	10
Turbine#2 outlet pressure of NG (MPa)	7
Turbine outlet pressure of argon (MPa)	1.44
Turbine outlet pressure of nitrogen (MPa)	2.93
Pinch point of the heat exchanger#1 (K)	2

Pinch point of the heat exchanger#2 (K)	2
Isentropic efficiency of the compressor [32]	75%
Isentropic efficiency of the cryo-pump/pump [24]	75%
Isentropic efficiency of the turbine#1&2 [28]	90%
Mass flow rate of working fluid (kg/s)	1

3.1 Selection of working fluid

In the LAES system, Dowtherm G (a type of thermal oil) is used to recover and store the compression heat due to its proper temperature range and good heat transfer performance. Thus, in this proposed LNG-based power generation system, Dowtherm G is used as the heat transfer medium of the heat source in the heat exchanger #1.

Normally, LNG needs to be pressurized before regasification to ensure the long-distance and high-efficiency NG pipeline transportation. Thus, in this proposed power generation system, LNG is pumped to high pressure (10 MPa) before entering the heat exchanger #2. The pressurized LNG is used to cool down the working fluid through its regasification process in the heat exchanger #2, after which it would be further heated to ambient temperature and then expanded in turbine#2 to 7 MPa for long distance transmission.

In the cryogenic power generation cycle, nitrogen and argon are widely used as the working fluid because of its very low triple point, nonflammability, and non-pollution, etc. [5]. To utilize the high-grade cold energy of LNG more effectively, nitrogen and argon are working under different outlet pressure of the turbine (P_4), respectively. Thus, at their respective design pressures, the liquefaction temperatures of nitrogen and argon (nitrogen: 123.13 K at 2.93 MPa, argon: 123.15 K at 1.44 MPa) can be very close to the LNG temperature.

3.2 Constant heat source and constant low-temperature exergy source

To analyze the influence of pressure ratio of the inlet to outlet of the turbine#1 (P_3/P_4) on this power generation system performance, the heat source (thermal oil as the heat transfer medium) and low-temperature exergy source (LNG as the heat transfer medium) are assumed to be constant temperature source at first. In this case, the temperatures of the cold and heat sources always keep constant during the working process, which can avoid the influence of the temperatures and mass flows of the cold and heat sources on the system performance. There is no analysis about the performance of Power generation#2 in this section is because that when the low-temperature exergy source is assumed to be a constant temperature source, the power generation amount of Power generation#2 could not be calculated.

3.2.1 The effect of the turbine pressure ratio

To guarantee the reasonability of the comparison between argon and nitrogen, the turbine pressure ratios (P_3/P_4) for argon and nitrogen have the same variation range (2-40), which could be controlled by regulating the inlet pressure (P_3). Fig. 5 shows the effect of the pressure ratio of the turbine (P_3/P_4) on the specific power generation of Power generation#1 ($w_{net,PG1}$). As seen in Fig. 5, with the increase of the turbine pressure ratio (P_3/P_4) from 2 to 40, the specific power generation of Power generation#1 ($w_{net,PG1}$) increases first and then decreases consistently, for both argon and nitrogen as the working fluids. This is mainly because the increase of the turbine pressure ratio (P_3/P_4) contributes to the increase of the power generation of the turbine#1. However, it also indicates the increase of the inlet pressure of the turbine (P_3) and in turn the outlet pressure of the compressor (P_2), increasing the compressor pressure ratio (P_2/P_1) and further the increase of the power consumption of the compressor. On the initial growth of the turbine pressure ratio (P_3/P_4), the increase of the power generation is faster than that of the power consumption, making the specific power generation ($w_{net,PG1}$) go up first. However, with the continuous increase of the turbine pressure ratio (P_3/P_4), the growth rate of the power consumption accelerates and finally catches up with the growth rate of the power generation at a certain turbine pressure ratio, which makes the specific power generation ($w_{net,PG1}$) reach the peak. As the further increase of the turbine pressure ratio (P_3/P_4), the growth rate of the power consumption overtakes the growth rate of the power generation, leading to the decline of the specific power generation ($w_{net,PG1}$). In terms of the comparative results from Fig. 5, it could also be seen that within the range of the turbine pressure ratio (P_3/P_4) between 2 and 40, the specific power generation of nitrogen is higher than that of argon, suggesting that nitrogen performs better as the working fluid when the constant cold and heat sources are considered. Besides, from Fig. 5, it could also be seen that with the increase of the LNG outlet pressure of the cryo-pump (P_6), the specific power generations ($w_{net,PG1}$) of both nitrogen and argon go down. However, this effect is more obvious on nitrogen than argon. The reason for this result is mainly because the increase of the outlet pressure of the cryo-pump leads to the increase of the cryo-pump outlet temperature of the LNG (T_6) since the pressure and temperature of the LNG in the LNG tank is fixed. Therefore, the compressor inlet temperature of nitrogen and argon (T_1) goes up as well, which would cause an increase in the power consumption of the compressor.

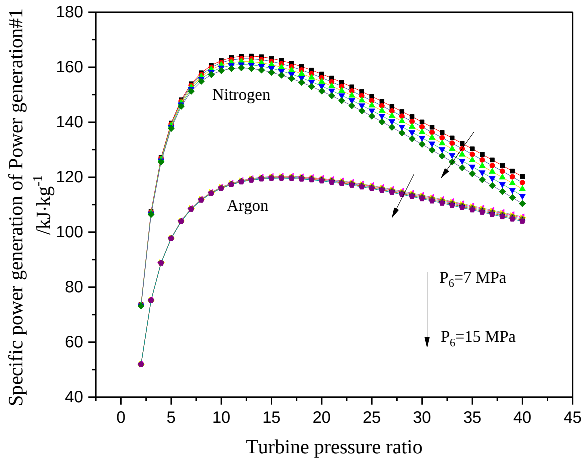

Fig. 5. The effect of the turbine pressure ratio on the specific power generation of nitrogen/argon at different LNG pressures (Power generation#1)

3.2.2 The effect of the hot source and low-temperature exergy source temperature

Besides, with the fixed turbine pressure ratio of 8 (P_3/P_4=8), the effects of the temperature of the constant heat and cold sources on the specific power generation ($w_{net,PG1}$) have been researched in detail. The temperature variation ranges of the low-temperature exergy source and the heat source are 113.15 K - 120.15 K and 413.15K - 473.15 K, respectively. Fig. 6 (a) and (b) show the variations of the specific power generations of Power generation#1 ($w_{net,PG1}$) as the change of the temperatures of the cold and heat sources, for argon and nitrogen as the working fluids respectively. The results illustrate that the lower low-temperature exergy source temperature and the higher heat source temperature could contribute to the increase of the specific power generation of Power generation#1. Furthermore, the influence strength of the temperatures of the cold and heat sources are different. According to Fig. 6 (a), it could be seen that as the low-temperature exergy source temperature (T_6) increases from 113.15K to 120.15K, 3.35% of the exergy loss occurs, resulting in 2.91% of the specific power generation of nitrogen decrease. Decreasing the heat source temperature from 473.15K to 413.15K, which indicates 51.7% of the exergy loss, leads to 18.0% of the specific power generation of nitrogen decrease. Thus, the change of the specific power generation caused by the change of the low-temperature exergy source temperature is ~2.49 times of that caused by the change of the heat source temperature, suggesting that for nitrogen as the working fluid, the effect of the low-temperature exergy source temperature on the system performance is stronger than that of the heat source temperature. However, the result is opposite when argon is used as the working fluid, shown in Fig. 6 (b). A cold exergy loss of 3.35% and a heat exergy loss of 51.7% decrease the specific power generation of argon by 0.50% and 15.5%, respectively. The decrease of the specific power generation of argon caused by the heat exergy loss is ~2.01 times of that caused by the cold exergy loss.

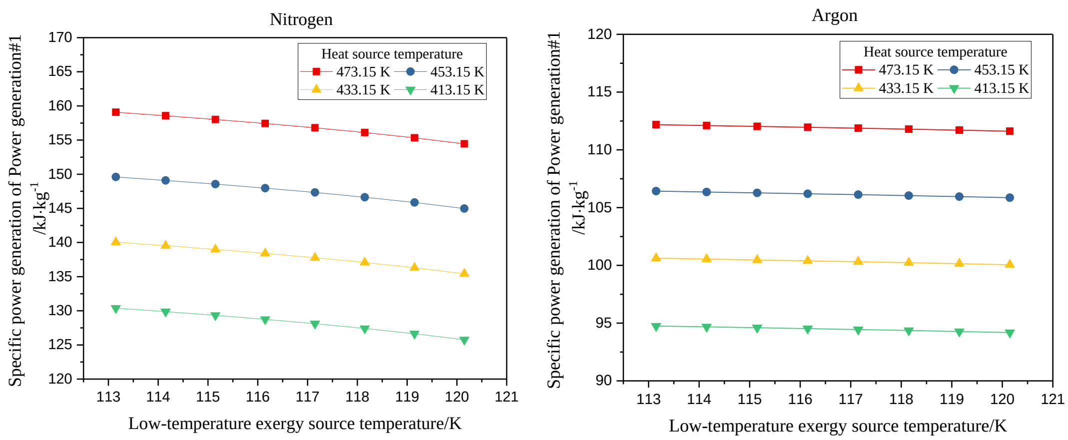

(a) (b)

Fig. 6. The effects of the hot source and low-temperature exergy source temperatures on the specific power generation of nitrogen (a) and argon (b) (Power generation#1)

3.3 Limited low-temperature exergy source and constant heat source

3.3.1 The effect of the mass flow rate of LNG-energy analysis

To analyze the effect of the mass flow rate of the cold fluid (LNG) on the system performance, the heat source is still assumed to be infinite and constant, whereas the mass flow rate of LNG is considered during the simulation process. The pressure ratio of the turbine is selected as 8 ($P_3/P_4 = 8$) and the LNG outlet pressure of the cryo-pump is fixed at 10 MPa (P_6=10 MPa). Fig. 7 shows the variations of the specific power generation of the nitrogen and argon of the whole system (w_{net}) and Power generation#1($w_{net,PG1}$) as the increase of the mass flow rate of LNG. Fig. 8 (a) and (b) show the T-S diagrams for nitrogen and argon during the entire power generation cycle, respectively. Since the heat source is assumed to be constant, the outlet state of the heat exchanger#1 (Status 3) is independent of the mass flow rate of LNG, which indicates Status 3 of this power generation cycle is settled. Based on Formula (4), the outlet condition of the turbine (Status 4) is settled as well. Therefore, the mass flow ratio of LNG to working fluid (K_{LNG}) could only influence the positions of Status 1 and Status 2 in T-S diagrams, while the positions of Status 3 and Status 4 are fixed.

From the nitrogen curves (red solid curve and red dashed curve) shown in Fig. 7, it could be observed that with the increasing mass flow ratio of LNG to the nitrogen (K_{LNG}), the specific power generation of Power generation#1 ($w_{net,PG1}$) rises when the ratio is smaller than 0.75 (K_{LNG} <0.75), beyond which (K_{LNG} >0.75), the growth trend slows down gradually and levels off finally. The final maximum specific power generation of Power generation#1 ($w_{net,PG1}$) approaches the value obtained when both the cold and heat sources are assumed to be constant. That is mainly because when the mass flow ratio of LNG to the nitrogen is below 0.75 (K_{LNG} <0.75), the cooling capacity is not enough to make the nitrogen condense in the heat exchanger #2. In this case, nitrogen in this power generation system could only finish the Brayton Cycle but not the Rankine Cycle. In this paper, this ratio value of 0.75 is defined as the cut off value of the Brayton Cycle of nitrogen. When the mass flow ratio is right equal to the cut off value (K_{LNG} = 0.75), nitrogen could complete the maximum-range Brayton Cycle, as shown in Fig. 8 (a): 1(a)-2(a)-3-4-1(a). When the mass flow ratio of LNG to nitrogen is over the cut off value (K_{LNG} > 0.75), nitrogen in this power generation system enters into the transition stage from the Brayton Cycle to Rankine Cycle. A growing part of the nitrogen could condense in the heat exchanger #2, but still some of the nitrogen remains gaseous state at the outlet of the heat exchanger #2. Until the mass flow ratio reaches 4.8 (K_{LNG} = 4.8), this power generation system can operate under the Rankine Cycle fully with nitrogen as the working fluid, as shown in Fig. 8 (a): 1(b)-2(b)-3-4-1(b). At the end, when the mass flow ratio is beyond 4.8 (K_{LNG} > 4.8), the specific power generation of nitrogen of Power generation#1 ($w_{net,PG1}$) can only get close to but not exceed the result calculated under the condition of constant low-temperature exergy source because of the pinch point constraint, as shown in Fig. 8 (a): 1(c)-2(c)-3-4-1(c). Besides, the red solid curve in Fig. 7 shows that the total specific power generation of the whole system (w_{net}) keeps rising with the increase of the mass flow rate of LNG, which is because that the increase of the mass flow rate of LNG could always contribute to the increase of the power generation of Power generation#2.

Also, the argon curves (blue solid curve and blue dashed curve) illustrated in Fig. 7 shows a very similar variation trend as the nitrogen curve, illustrating the cut off value of the Brayton Cycle for argon in this power generation system is 0.15 (K_{LNG} = 0.15). When the mass flow ratio of LNG to the argon is not higher than 0.15 (K_{LNG} ≤ 0.15), the power generation#1 can only work under the Brayton Cycle, showing a fast-rising trend of the specific power generation of argon of power generation#1. When the ratio is between 0.15 and 8.50 (0.15 < K_{LNG} < 8.50), an increasing amount of argon could finish the transition from the Brayton Cycle to the Rankine Cycle, as present in Fig. 8 (b): from 1(a)-2(a)-3-4-1(a) to 1(b)-2(b)-3-4-1(b). During this transition stage, the increasing rate of the specific power generation of argon of power generation#1 slows down. When the ratio overtakes 8.50 ($K_{LNG} \geq 8.50$), argon in this power generation system could complete the full Rankine Cycle and the specific power generation of argon of power generation#1 shows a level-off gradually, as illustrated in Fig. 8 (b): from 1(b)-2(b)-3-4-1(b) to 1(c)-2(c)-3-4-1(c). Furthermore, it could also be seen that the total specific power generation of the whole system (w_{net}) keeps increasing due to the increasing power generation contribution of Power generation#2.

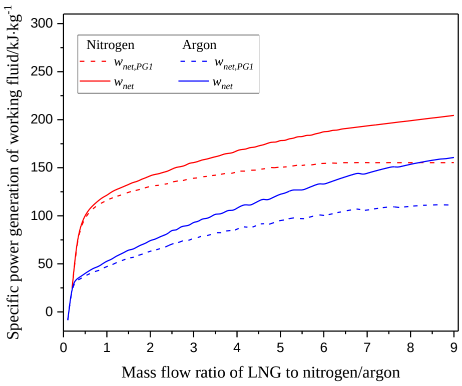

Fig. 7. Specific power generation variation with the mass flow ratio of LNG to nitrogen/argon (Power generation#1 and whole system)

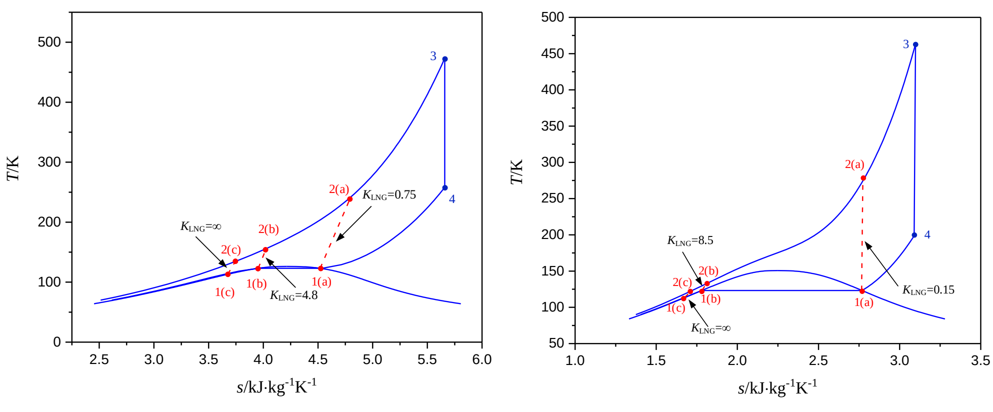

(a) (b)

Fig. 8. T-S diagrams for (a) nitrogen and (b) argon.

Furthermore, given the consumption of LNG, the power generation per unit mass flow of LNG for Power generation#1 ($w_{net,PG1}^{LNG}$) and the whole system (w_{net}^{LNG}) are also be calculated, shown in Fig. 9. It can be seen that the power generations per unit mass flow of LNG ($w_{net,PG1}^{LNG}$ and w_{net}^{LNG}) have a totally different variation trend with the specific power generations ($w_{net,PG1}$ and w_{net}). They rise to the peak at the mass flow ratios of 0.30 and 0.20 (K_{LNG} = 0.30 and 0.20), when nitrogen and argon are used as the working fluid, respectively. After the peak, the power generation per unit mass flow of LNG for both Power generation#1 ($w_{net,PG1}^{LNG}$) and the whole system (w_{net}^{LNG}) show a sharp decline firstly and then change little gradually. Fig. 10. (a) and (b) show the peak composite curves of the heat exchanger#2 with nitrogen and argon as the working fluid, respectively, suggesting a highly efficient utilization of the cold energy of LNG. Therefore, in terms of the utilization efficiency of the cold energy of LNG, rather than the more the better, there is an optimal value of the mass flow rate of LNG in this power generation system. In addition, for nitrogen as the working fluid, the Brayton Cycle is the most effective and efficient option for this power generation system, given the result of Fig. 10 (a). However, for argon as the working fluid, the combination of the Brayton Cycle and Rankine Cycle (argon has a vapor fraction of 97.10% at the outlet of the heat exchanger #2) is the most beneficial way, based on the result of Fig. 10 (b).

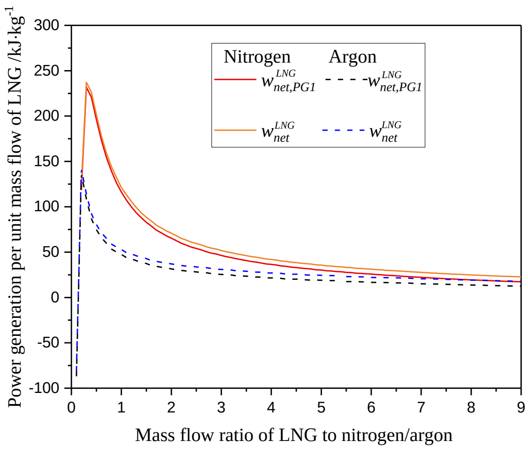

Fig. 9 Effect of the mass flow ratio of LNG to nitrogen/argon on power generation per unit mass flow of LNG (Power generation#1 and whole system)

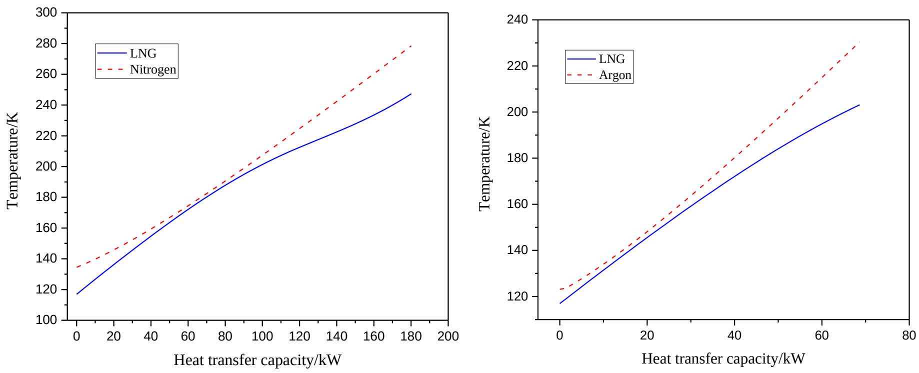

(a) (b)

Fig. 10. Composite curves of the heat exchanger #2 with nitrogen (a) and argon (b) as working fluids.

3.3.2 The effect of the mass flow rate of LNG-exergy analysis

The influence of the mass flow rate of LNG on the total system exergy destruction (Ex_d) and the exergy destruction per unit mass flow rate of LNG (Ex_d^{LNG}) is also studied through the exergy analysis, illustrating in Fig. 11. The total exergy destruction (Ex_d, blue curves) almost keeps constant at the very beginning of the increase of LNG input to the whole system, and then increases sharply with the continuous rise of the LNG amount. Thus, the exergy destructions per unit mass flow rate of LNG (Ex_d^{LNG}, red curves) have minimum values at the mass flow ratios of 0.30 and 0.20 (K_{LNG} = 0.30 and 0.20) for nitrogen and argon, respectively. From the exergy destruction comparison between nitrogen and argon in Fig. 11, it could be found that with the same LNG input amount, Argon always has a higher system exergy destruction. Fig. 12 shows the respective exergy destructions of Power generation#1 and 2 ($Ex_{d,PG1}^{LNG}$ and $Ex_{d,PG2}^{LNG}$), illustrating that the sharp decrease of the total exergy destruction per unit mass flow rate of LNG at the very beginning of the increase of LNG input is mainly caused by the sharp decrease of the exergy destruction of Power generation#1. For Power generation#2, the exergy destruction per unit mass flow rate of LNG goes up first and finally almost keeps unchanged, and this result is mainly decided by the exergy destruction variation trend of the ambient heat exchanger.

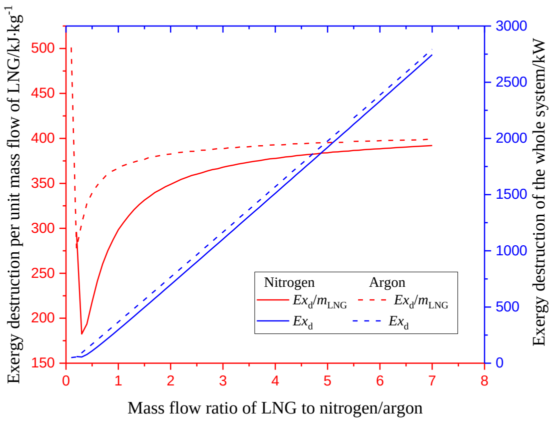

Fig. 11 Effect of the mass flow ratio of LNG to nitrogen/argon on exergy destruction

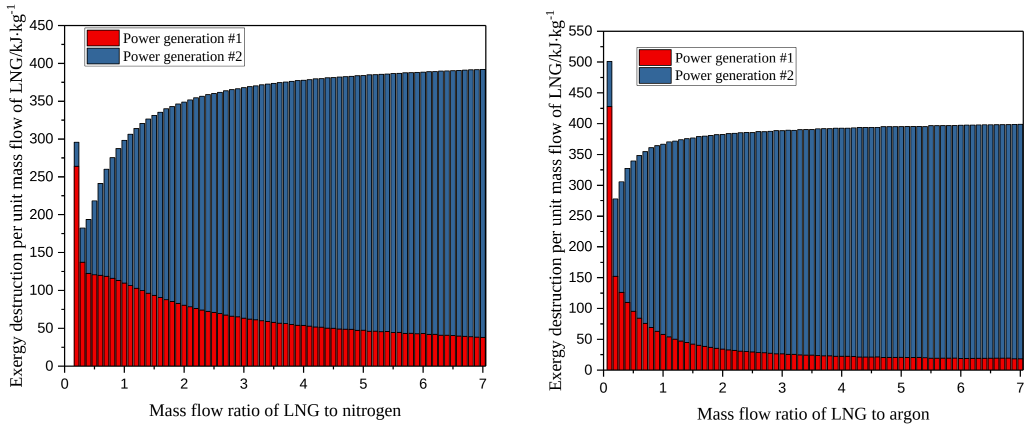

(a) (b)

Fig. 12 Exergy destruction distribution in Power generation#1 and 2 with nitrogen (a) and argon (b) as working fluids.

3.4 Limited cold and heat sources

3.4.1The effect of the mass flow rate of thermal oil-energy analysis

Besides the mass flow rate of LNG, the mass flow of the heat source (high-temperature thermal oil) is also one of the key influential factors of the system performance. Thus, the effects of this factor on the specific power generation (w_{net}) and power generation per unit thermal oil (w_{net}^{oil}) are investigated and the results are illustrated in Fig. 13 and Fig. 14, respectively. The best mass flow ratios of LNG to nitrogen/argon obtained in section 3.3 (K_{LNG}=0.30 and 0.20, respectively) are employed and fixed in this section.

It could be seen from Fig. 13 that as the increasing mass ratio of the thermal oil to nitrogen/argon (K_{oil}), the specific power generation of Power generation#1 ($w_{net,PG1}$) goes up to the maximum at first and then stays constant. The turning points from the rising trend to level-off are 0.75 and 0.35 for nitrogen and argon, respectively. That is because there is an upper limit on the outlet temperature of the heat exchanger #1 which is determined by the heat source temperature and the pinch point of the heat exchanger. The initial increase of the mass flow of thermal oil could raise the working fluid temperature at the outlet of the heat exchanger #1. However, once the outlet temperature reaches the upper limit, the continuous increase of the mass flow of the thermal oil would no longer affect the outlet status of the heat exchanger #1 (Status 3). Besides, the Status 4 and the specific power generation ($w_{net,PG1}$) are fixed as well after the turning point according to the formula (4) and (11)-(15) since Status 3 is settled. As for the power generation per unit mass flow of the thermal oil of Power generation#1 ($w_{net,PG1}^{oil}$), it has a peak value at their respective turning points (K_{oil} = 0.75 for nitrogen and K_{oil} = 0.35 for argon), shown in Fig. 14. As for the specific power generation and power generation per unit mass flow of the thermal oil of the whole system (w_{net} and w_{net}^{oil}), they have the same variation trends as the those of Power generation#1 because the input amount of the thermal oil almost does not have any influence on the performance of Power generation#2.

Furthermore, the thermal efficiencies of Power generation#1 and the whole system ($\eta_{th,PG1}$ and η_{th}) are also studied and shown in Fig. 15. The variation trend of the thermal efficiencies ($\eta_{th,PG1}$ and η_{th}) are very similar with the specific power generation ($w_{net,PG1}$ and w_{net}), further illustrating that there is an optimal mass flow rate of the heat source for this power generation system (K_{oil} = 0.75 for nitrogen and K_{oil} = 0.35 for argon), which can maximize the thermal efficiency the specific power generation and the power generation per unit mass flow of the thermal oil of both Power generation#1 and the whole system, at the same time. In addition, the thermal efficiency of the Power generation#1 ($\eta_{th,PG1}$) and the whole system (η_{th}) are close for nitrogen as the working fluid, while the thermal efficiency of the Power generation#1 ($\eta_{th,PG1}$) is much higher than that of the whole system (η_{th}) for argon as the working fluid, due to the different heat input through the ambient heat exchanger ($Q_{hot,PG2}$) in argon and nitrogen systems. After the first-stage regasification process in Heat exchanger#2, the LNG inlet temperature of the ambient heat exchanger (T_7) is still much lower than the ambient temperature in the argon system, shown in Fig. 10 (b), which leads to a much higher heat input through the ambient heat exchanger ($Q_{hot,PG2}$) than the nitrogen system, and then leads to the lower thermal efficiency of the whole system (η_{th}).

Fig. 16 shows the composite curves for the heat exchanger #1 under the condition of the highest thermal efficiency. It could be seen that the temperature gradients of the working fluids (nitrogen and argon) and thermal oil in each of the heat exchangers could match well with the constraints at the pinch point, suggesting highly effective heat exchangers.

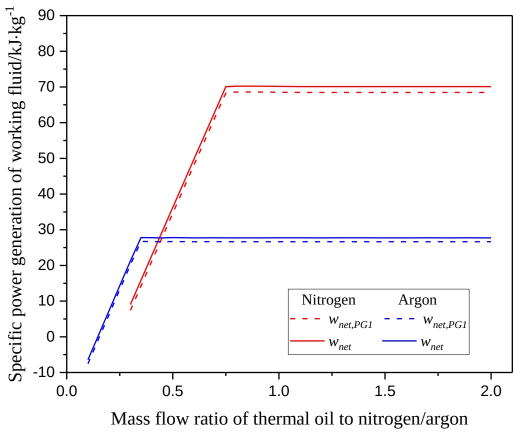

Fig. 13. Specific power generation variation with the mass flow ratio of thermal oil to nitrogen/argon (Power generation#1 and whole system)

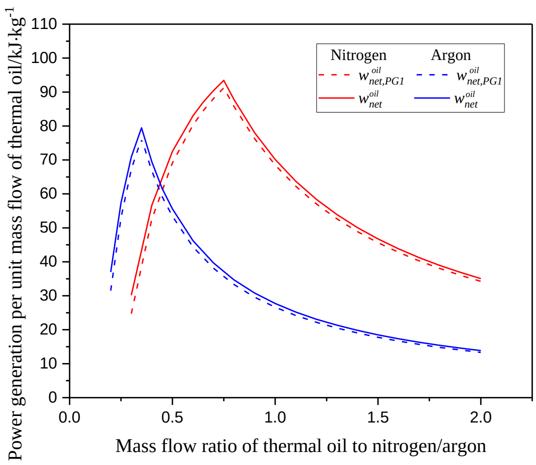

Fig. 14. Effect of the mass flow ratio of thermal oil to nitrogen/argon on power generation per unit mass flow of thermal oil (Power generation#1 and whole system)

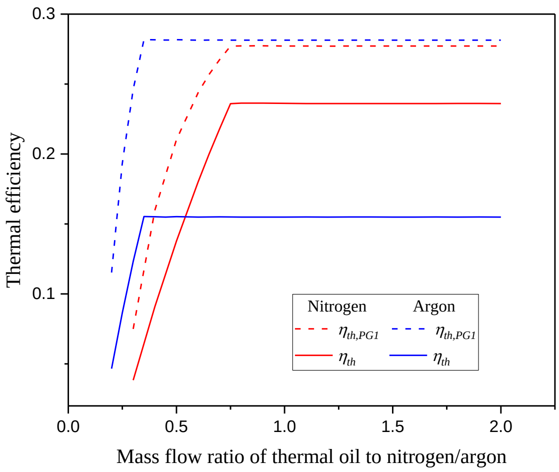

Fig. 15. Effect of the mass flow ratio of thermal oil to nitrogen/argon on thermal efficiency (Power generation#1 and whole system)

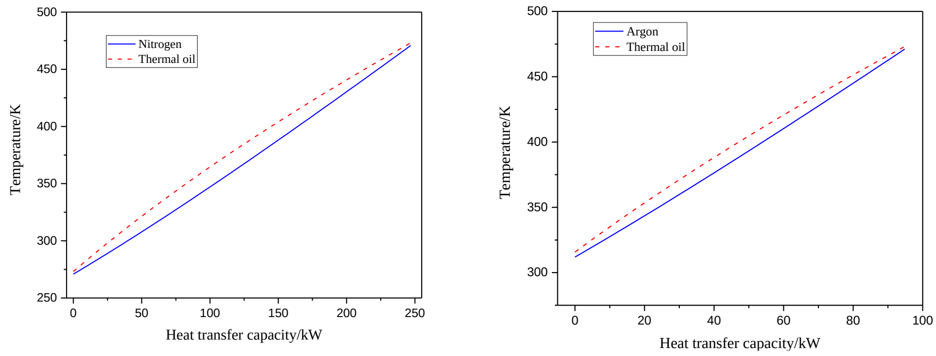

(a) (b)

Fig. 16. Composite curves of heat exchanger #1 with nitrogen (a) and argon (b) as working fluids.

3.4.2 The effect of the mass flow rate of thermal oil-exergy analysis

The exergy analysis is also carried out in this section. Fig. 17 and Fig. 18 show the effect of the mass flow rate of the thermal oil on the exergy efficiency and the exergy destruction distribution, respectively. The highest exergy efficiency occurs at the same point when thermal efficiency reaches the maximum value (K_{oil} = 0.75 for nitrogen and K_{oil} = 0.35 for argon), illustrated in Fig. 17. Besides, the exergy efficiency of the nitrogen system is much higher than the argon system, suggesting that using nitrogen as the working fluid is a better way to recover the waste compression heat of LAES and cryogenic energy of LNG. From Fig. 18 could be seen that with the increase of the mass flow rate of the thermal oil, the total exergy destruction of the whole system decreases first due to the obvious decrease of the exergy destruction in the ambient heat exchanger. Then, the total exergy destruction of the whole system reaches the minimum value (K_{oil} = 0.75 for nitrogen and K_{oil} = 0.35 for argon) after which the total exergy destruction goes up mainly due to the exergy destruction increase in heat exchanger#1.

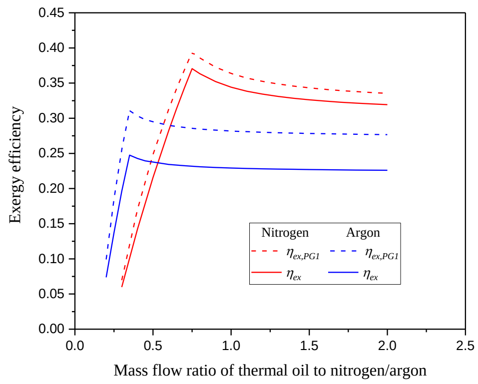

Fig. 17 Effect of the mass flow ratio of thermal oil to nitrogen/argon on exergy efficiency (Power generation#1 and whole system)

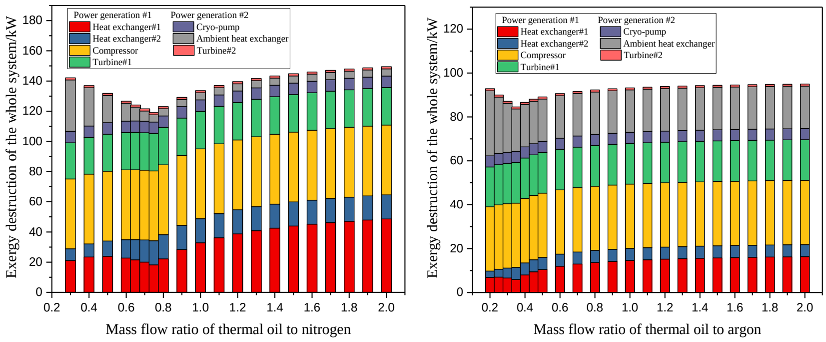

(a) (b)

Fig. 18 Exergy destruction distribution in each component of the whole system with nitrogen (a) and argon (b) as working fluids.

3.4.3 The effect of the pressure drop of heat exchangers

In the discussions above, the pressure drops in all heat exchangers of this proposed power generation system are neglected. However, the pressure drop of heat exchangers is also a very important influence factor on system performance. Thus, in this section, with the fixed mass flow rate of both thermal oil and LNG (nitrogen: K_{LNG}=0.30 and K_{oil} = 0.75; argon: K_{LNG}= 0.20 and K_{oil} = 0.35), the effect of the pressure drop is studied, which is illustrated in Fig. 19. In could be seen from the result in Fig. 19 that as the pressure drop increases from 0% to 2.0%, the total exergy input of the whole system (orange line) almost keeps constant, while the total exergy destruction of the whole system (green line) goes up, reducing the total net energy output and the exergy efficiency of the whole system. The main reason for the increase of the total exergy destruction is because the increase of the pressure drop leads to more exergy destruction in every heat exchange component. The results indicate that the 1% increase of the pressure drop could lead to ~3.5% and ~7% decrease of the whole system exergy efficiency, for nitrogen and argon as working fluids, respectively.

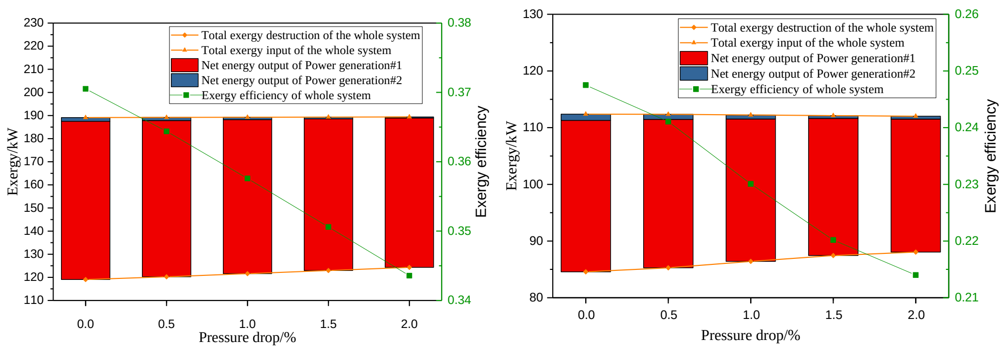

(a) (b)

Fig. 19 Effect of the pressure drop of heat exchangers on the system performance with nitrogen (a) and argon (b) as working fluids

4. Economic evaluation

As detailed in the previous sections, nitrogen is a better option to be used as the working fluid in this proposed power generation system, which could have a higher specific net power output, thermal efficiency, and exergy efficiency. It would be of interest to evaluate the economic benefits to invest this extra power generation system with nitrogen as the working fluid as the subsidiary system for an LAES system and an LNG terminal. Since all configurations in power generation#2 stays the same as the original LNG regasification configurations in the LNG terminal, the economic analysis is based on the total generated electricity earning and the capital investment cost of the power generation#1. The cost functions for all the components in the power generation#1 are shown in Table 6.

Table 6 cost functions for Economic analysis

System components	Capital investment cost function	Original year	CEPCI
Turbine [33]	$\frac{479.34\cdot m}{0.92\text{-}\eta_{tur}}\cdot\ln(\frac{P_{in}}{P_{out}})\cdot\left(1+e^{0.036T_i-54.4}\right)$	1996	381.7
Compressor [33]	$\frac{71.1\cdot m}{0.9\text{-}\eta_{com}}\cdot\frac{P_{out}}{P_{in}}\cdot\ln(\frac{P_{out}}{P_{in}})$	1996	381.7
Heat exchanger [34]	$1650\left\{\frac{q_{HX}(1/htc_c+1/htc_h)}{\left[\Delta t_{in}\Delta t_{out}(\frac{\Delta t_{in}+\Delta t_{out}}{2})\right]^{1/3}}\right\}^{0.65}$	2001	394.3

Cost indices are required to convert purchased equipment cost into one that is accurate for the present time. In this work, the chemical engineering plant cost index (CEPCI) is referred to adjust for the effects of inflation through time. Besides the operating and maintenance costs typically amount to between 1.5% and 3% of the capital cost of the whole system per annum [35]. In this paper, the O&M cost is assumed to account for 2% of the capital cost per annum.

According to [23], there is about 395 ton/day thermal oil could not be used for a stand-alone LAES system (scale: 5MW/40MWh). In [23], an ORC system with R32 as the working fluid is proposed to recover this part of excess heat for power generation (ambient temperature cooling water is used for condensation). For comparison, an LAES system (scale: 5MW/40MWh) is assumed to be integrated with the LNG regasification process in the way proposed in this paper, and all of this excess thermal oil is utilized for power generation with nitrogen as the working fluid. In the analysis, the charging process of the LAES runs at off-peak time for 8 hours per day and 300 days per year, hence, the power generation#1 could work for the rest of 16 hours in the same day (8 hours each in peak and off-peak time) at a rated power of 626 kW. The rates of electricity of $291/MWh during peak time, $80.6/MWh during off-peak time, the discount rate of 5% and the lifespan of 15 years are used in the calculation process, all of which are the same as [23] for comparison purpose. The results are shown in Table 7. It could be seen that the proposed power generation system in this paper is more excellent with a payback period of only 2.19 years and a saving to investment ratio of 4.73, suggesting that it is a more economical way to build a waste energy-based power plant co-located with the LNG terminal and LAES plant than to build a waste energy-based power plant only located with LAES plant alone. Besides, in this case, the specific investment cost of this waste energy-based power plant co-located with the LNG terminal and LAES plant is 1877 $/kW approximately.

Table 7 Economic analysis comparative results

Performance indexes	System in this paper	System in [23]
Saving to investment ratio	4.73	2.78
Net present value ($)	4,379,880	2,690,991
Payback period (years)	2.19	3.1

Furthermore, the effect of the peak electricity tariff on the economic benefit has been considered when the off-peak time electricity tariff is fixed at $80.6/MWh, illustrated in Fig. 20. It could be seen that when there is no price difference between the peak and off-peak electricity, the payback period is 5.3 years, and higher price difference between the peak and off-peak electricity could reduce the payback period very obviously.

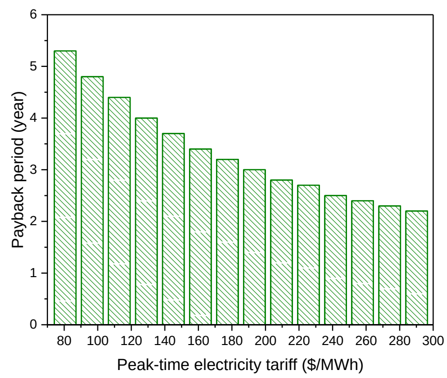

Fig. 20 Effect of peak electricity tariff on the payback period

5. Conclusions

In this paper, a power plant for recovering the high-grade cold energy from LNG (-160 ºC) and waste compression heat from the LAES system (200 ºC) is proposed, which provides a new thought in the integration methods between the LAES system and the LNG regasification process. Through this way, the LAES system could keep the same configurations with the existing LAES pilot plant and grid-scale demonstration plant, and very less reconstruction work is needed by the original LNG terminal, making it more industrially feasible.

Nitrogen and argon are selected as the working fluids. Both energy analysis and exergy analysis are conducted on this power plant under different working conditions to optimize the working parameters for nitrogen and argon, respectively, filling the gap in designing power plants working in a wide temperature range. Some conclusions have been obtained as follows:

- The optimal mass flow rate ratios of the working fluid to LNG to thermal oil are achieved, which are 1:0.3:0.75 and 1:0.2:0.3 for this power generation system with nitrogen and argon as working fluids, respectively. With the optimal mass flow ratio, the power generation per unit mass flow of LNG and thermal oil, thermal efficiency (nitrogen: ~27% and argon: ~19%) and exergy efficiency (nitrogen: ~40% and argon: ~28%) of this system could all reach the maximum value, suggesting the best utilization of both the waste compression heat and cryogenic energy under the given design condition.
- Nitrogen is more suitable to work in this proposed power generation system than argon, given both the thermal efficiency and exergy efficiency of the whole system (Power generation #1 and 2). However, argon has a higher thermal efficiency in stand-alone Power generation#1.
- Every 1% increase of the pressure drop in heat exchangers could lead to ~3.5% and ~7% decrease of the whole system exergy efficiency, for nitrogen and argon as working fluids, respectively.
- Under given circumstances, a waste energy-based power plant co-driven by the excess heat from an LAES power plant (5MW/40MWh) and the waste cold from an LNG supply terminal could achieve a payback period of 2.19 years and a saving to investment ratio of 4.73, which is more economical than a waste energy-based power plant only driven by the LAES excess heat.

The analyses of this work suggest that a newly LAES system is more recommended to be built nearby an existing LNG supply terminal to reutilize its excess heat more profitably, benefiting both the

LAES and LNG side.

Reference

[1] U.S. Energy Information Administration. EIA - International Energy Outlook 2017. Int Energy Outlook 2017 2017:76. doi:www.eia.gov/forecasts/ieo/pdf/0484(2016).pdf.

[2] Dutta A, Karimi IA, Farooq S. Economic Feasibility of Power Generation by Recovering Cold Energy during LNG (Liquefied Natural Gas) Regasification. ACS Sustain Chem Eng 2018;6:10687–95. doi:10.1021/acssuschemeng.8b02020.

[3] Karimi IA, Khan MS. Special Issue on PSE Advances in Natural Gas Value Chain: Editorial. Ind Eng Chem Res 2018;57:5733–5. doi:10.1021/acs.iecr.8b01543.

[4] Kanbur BB, Xiang L, Dubey S, Choo FH, Duan F. Cold utilization systems of LNG: A review. Renew Sustain Energy Rev 2017;79:1171–88. doi:10.1016/j.rser.2017.05.161.

[5] Li Y, Chen H, Ding Y. Fundamentals and applications of cryogen as a thermal energy carrier: A critical assessment. Int J Therm Sci 2010;49:941–9. doi:10.1016/j.ijthermalsci.2009.12.012.

[6] Chen H, Cong TN, Yang W, Tan C, Li Y, Ding Y. Progress in electrical energy storage system: A critical review. Prog Nat Sci 2009;19:291–312. doi:10.1016/j.pnsc.2008.07.014.

[7] Morgan R, Nelmes S, Gibson E, Brett G. Liquid air energy storage - Analysis and first results from a pilot scale demonstration plant. Appl Energy 2015;137:845–53. doi:10.1016/j.apenergy.2014.07.109.

[8] Brett G, Barnett M. Utility-scale energy storage: Liquid air a pioneering solution to the problem of energy storage. IET Semin. Dig., vol. 2013, 2013. doi:10.1049/ic.2013.0129.

[9] She X, Li Y, Peng X, Ding Y. Theoretical analysis on performance enhancement of stand-alone liquid air energy storage from perspective of energy storage and heat transfer. Energy Procedia, vol. 142, Elsevier Ltd; 2017, p. 3498–504. doi:10.1016/j.egypro.2017.12.236.

[10] Peng X, She X, Li C, Luo Y, Zhang T, Li Y, et al. Liquid air energy storage flexibly coupled with LNG regasification for improving air liquefaction. Appl Energy 2019;250:1190–201. doi:10.1016/j.apenergy.2019.05.040.

[11] Park J, You F, Cho H, Lee I, Moon I. Novel massive thermal energy storage system for liquefied natural gas cold energy recovery. Energy 2020;195. doi:10.1016/j.energy.2020.117022.

[12] Park J, Lee I, Yoon H, Kim J, Moon I. Application of Cryogenic Energy Storage to Liquefied Natural Gas

Regasification Power Plant. Comput. Aided Chem. Eng., vol. 40, Elsevier B.V.; 2017, p. 2557–62. doi:10.1016/B978-0-444-63965-3.50428-1.

[13] Park J, Lee I, Moon I. A Novel Design of Liquefied Natural Gas (LNG) Regasification Power Plant Integrated with Cryogenic Energy Storage System. Ind Eng Chem Res 2017;56:1288–96. doi:10.1021/acs.iecr.6b04157.

[14] Park J, Cho S, Qi M, Noh W, Lee I, Moon I. Liquid Air Energy Storage Coupled with Liquefied Natural Gas Cold Energy: Focus on Efficiency, Energy Capacity, and Flexibility. Energy 2020:119308. doi:10.1016/j.energy.2020.119308.

[15] Zhang T, Chen L, Zhang X, Mei S, Xue X, Zhou Y. Thermodynamic analysis of a novel hybrid liquid air energy storage system based on the utilization of LNG cold energy. Energy 2018;155:641–50. doi:10.1016/j.energy.2018.05.041.

[16] Luyao L, Sixian W, Zhang D, Luwei Y, Yuan Z, Junjie W. Performance analysis of liquid air energy storage utilizing LNG cold energy. IOP Conf. Ser. Mater. Sci. Eng., 2017. doi:10.1088/1757-899X/171/1/012032.

[17] Kim J, Noh Y, Chang D. Storage system for distributed-energy generation using liquid air combined with liquefied natural gas. Appl Energy 2018;212:1417–32. doi:10.1016/j.apenergy.2017.12.092.

[18] Hamdy S, Morosuk T, Tsatsaronis G. Exergetic and economic assessment of integrated cryogenic energy storage systems. Cryogenics (Guildf) 2019;99:39–50. doi:10.1016/j.cryogenics.2019.02.009.

[19] Lee I, Park J, Moon I. Conceptual design and exergy analysis of combined cryogenic energy storage and LNG regasification processes: Cold and power integration. Energy 2017;140:106–15. doi:10.1016/j.energy.2017.08.054.

[20] Lee I, You F. Systems design and analysis of liquid air energy storage from liquefied natural gas cold energy. Appl Energy 2019;242:168–80. doi:10.1016/j.apenergy.2019.03.087.

[21] Lee I, Park J, You F, Moon I. A novel cryogenic energy storage system with LNG direct expansion regasification: Design, energy optimization, and exergy analysis. Energy 2019;173:691–705. doi:10.1016/j.energy.2019.02.047.

[22] She X, Zhang T, Cong L, Peng X, Li C, Luo Y, et al. Flexible integration of liquid air energy storage with liquefied natural gas regasification for power generation enhancement. Appl Energy 2019;251. doi:10.1016/j.apenergy.2019.113355.

[23] She X, Peng X, Nie B, Leng G, Zhang X, Weng L, et al. Enhancement of round trip efficiency of liquid

air energy storage through effective utilization of heat of compression. Appl Energy 2017;206:1632–42. doi:10.1016/j.apenergy.2017.09.102.

[24] Peng X, She X, Cong L, Zhang T, Li C, Li Y, et al. Thermodynamic study on the effect of cold and heat recovery on performance of liquid air energy storage. Appl Energy 2018;221:86–99. doi:10.1016/j.apenergy.2018.03.151.

[25] She X, Zhang T, Peng X, Wang L, Tong L, Luo Y, et al. Liquid Air Energy Storage for Decentralized Micro Energy Networks with Combined Cooling, Heating, Hot Water and Power Supply. J Therm Sci 2020;29:1–17. doi:10.1007/s11630-020-1396-x.

[26] Marmolejo-Correa D, Gundersen T. A comparison of exergy efficiency definitions with focus on low temperature processes. Energy 2012;44:477–89. doi:10.1016/j.energy.2012.06.001.

[27] Kotas TJ. EXERGY CRITERIA OF PERFORMANCE FOR THERMAL PLANT. Int J Heat Fluid Flow 1980;2:147–63. doi:10.1016/0142-727X(80)90010-7.

[28] Bao J, Lin Y, Zhang R, Zhang N, He G. Strengthening power generation efficiency utilizing liquefied natural gas cold energy by a novel two-stage condensation Rankine cycle (TCRC) system. Energy Convers Manag 2017;143:312–25. doi:10.1016/j.enconman.2017.04.018.

[29] Li C, Liu J, Zheng S, Chen X, Li J, Zeng Z. Performance analysis of an improved power generation system utilizing the cold energy of LNG and solar energy. Appl Therm Eng 2019;159. doi:10.1016/j.applthermaleng.2019.113937.

[30] Tsougranis EL, Wu D. A feasibility study of Organic Rankine Cycle (ORC) power generation using thermal and cryogenic waste energy on board an LNG passenger vessel. Int. J. Energy Res., vol. 42, 2018, p. 3121–42. doi:10.1002/er.4047.

[31] Aneke M, Agnew B, Underwood C. Performance analysis of the Chena binary geothermal power plant. Appl Therm Eng 2011;31:1825–32. doi:10.1016/j.applthermaleng.2011.02.028.

[32] Function Team M. Compressor Selection Guidelines. 2013.

[33] Mirmasoumi S, Khoshbakhti Saray R, Ebrahimi S. Evaluation of thermal pretreatment and digestion temperature rise in a biogas fueled combined cooling, heat, and power system using exergo-economic analysis. Energy Convers Manag 2018;163:219–38. doi:10.1016/j.enconman.2018.02.069.

[34] Chen JJJ. Comments on improvements on a replacement for the logarithmic mean. Chem Eng Sci 1987;42:2488–9. doi:10.1016/0009-2509(87)80128-8.

[35] Xie C, Hong Y, Ding Y, Li Y, Radcliffe J. An economic feasibility assessment of decoupled energy storage in the UK: With liquid air energy storage as a case study. Appl Energy 2018;225:244–57. doi:10.1016/j.apenergy.2018.04.074.